Journal of Particle Science and Technology 9 (2) (2023) 51-61

Iranian Research Organization for Science and Technology (IROST)

Journal of PARTICLE Science & Technology

JPST
https://jpst.irost.ir

Online ISSN: 2423-4079
Print ISSN: 2423-4087

Heavy metal removal using SnO_2 nanoparticles prepared in a grape extract media

Saeid Jabbarzare

Advanced Materials Research Center, Department of Materials Engineering, Najafabad Branch, Islamic Azad University, Najafabad, Iran

HIGHLIGHTS

- The biosynthesis of SnO_2 nanoparticles using a grape extract media is reported.
- SnO_2 nanoparticles were characterized by XRD, FESEM, TEM, BET, and DLS techniques.
- SnO_2 nanoparticles were used as an efficient adsorbent for the removal of Pb^{2+} and Cd^{2+} ions from wastewater.
- The effect of different parameters including adsorbent dosage, Cd and Pb concentration, temperature, and on the adsorption was investigated.

GRAPHICAL ABSTRACT

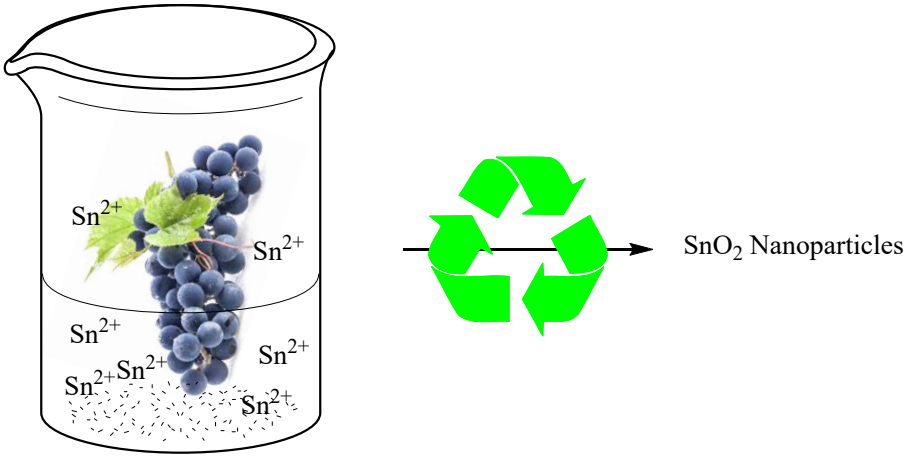

ARTICLE INFO

Article type:

Research article

Article history:

Received 7 July 2023
Received in revised form 17 November 2023
Accepted 18 November 2023

Keywords:

Removal of heavy metals
Grape extract
Kinetic and thermodynamic
Wastewater
SnO_2

DOI: 10.22104/JPST.2023.6385.1236

ABSTRACT

SnO_2 nanoparticles were first synthesized using a grape extract media, then characterized by XRD, FE-SEM, TEM, BET, and DLS techniques, and finally used as an efficient adsorbent for the removal of Pb^{2+} and Cd^{2+} ions from wastewater. The prepared sample had a tetragonal phase with an average crystallite size of 41 nm (XRD analysis), a specific surface area of 47.08 $m^2.g^{-1}$ (BET method)/46.25 $m^2.g^{-1}$ (BJH method), and a pore diameter of 6.49 nm (BJH method). The best conditions for adsorbing were a 30 ppm concentration of metal ions, ambient temperature, pH of 6, and 0.025 g of an adsorbent. The maximum adsorption for Pb and Cd ions was 97 and 93%, respectively. The Elovich model was matched as the most suitable kinetic model, indicating that the adsorption mechanism is chemical adsorption. The negative values of ΔG (Pb: -6.38 $kJ.mol^{-1}$; Cd: -4.16 $kJ.mol^{-1}$) represent the spontaneousness of the adsorption process. The negative values of the parameters ΔH (Pb: -63.0 $kJ.mol^{-1}$; Cd: -42.95 $kJ.mol^{-1}$) and ΔS (Pb: -188.8 $J.mol^{-1}$; Cd: -128.4 $J.mol^{-1}$) represent the exothermic nature of the adsorption.

✉ *Corresponding author: E-mail address:* saeid.jabbarzare@gmail.com ; *Tel:* +9831-42292630 ; *Fax:* +9831-42291016

1. Introduction

Due to their unique physical and chemical properties, Tin(IV) oxide (SnO_2) nanoparticles are used in industries, laboratories, and environmental sciences. SnO_2 has high chemical stability, high conductivity, and high catalytic activity. SnO_2 also has suitable optical and electrical properties due to its wide bandgap characteristics, which make it a good candidate for gas sensors and transparent conducting devices. It is known as an anode electrode in the electrolytic production of aluminum and lithium rechargeable batteries. Despite these good characteristics of SnO_2, they can be influenced, improved, or even changed depending on their preparation method, particle size, and morphology. For example, reducing SnO_2 crystalline size is very effective in improving gas sensitivity [1-7].

To date, various methods have been used for the preparation of SnO_2 nanostructures. Traditionally, SnO_2 is synthesized from the hydrolysis of Sn(IV) or Sn(II) salts at high temperatures [8]. The method and the raw materials used for the preparation of SnO_2 nanostructures determine the advantages of each method. Various methods, including co-precipitation and sol-gel methods, hydrothermal technique, microwave-assisted thermal decomposition, cracking, physical and chemical vapor deposition, and spray pyrolysis, have been used for the preparation of different structures of SnO_2 particles. These procedures suffer from various unwanted problems as they require high and complex operation costs and heavy and costly equipment and give uniform and too large particles. The chemical methods cause many challenges due to the use of hazardous and toxic chemicals and environmental damage [8-11]. Thus, nowadays, biological synthesis has been widely considered to improve the applicable characteristics of nanoparticles as well as reduce the environmental damage caused by chemical methods. While chemical methods lead to the survival of some toxic reactants, plant extracts are environmentally friendly and suitable for synthesizing nanoparticles due to reduced costs and lack of toxic substances. The use of herbal extracts as natural surfactants can be a good alternative to expensive synthetic surfactants [8-15].

Heavy metals such as cadmium and lead are usually defined as the most critical pollutants in the environment. Lead is toxic, and exposure to large amounts of it can cause mental retardation, behavioral disorders, and musculoskeletal problems. It also accumulates in various organs, especially in the brain, leading to toxicity and ultimately to human death. Cadmium is a potentially toxic heavy metal that can be integrated into the human body and remain in the human body for more than ten years [16].

Many methods are being used to remove heavy metal ions, including filtration, coagulation process, adsorption, oxidation, reverse osmosis, ion exchange, precipitation, etc. Among these methods, the adsorption process has been widely used due to the abundance and availability of adsorbents such as clay, activated carbon, zeolites, etc. [17]. In addition, the adsorption technique is widely used because it is a simple operation with low power consumption, easy maintenance, and greater efficiency for wastewater treatment [18].

In recent years, the use of nanomaterial sorbents has been increasing with remarkable results in pollution removal. Nanomaterials have a high surface area and more active sites to adsorb heavy metals [19]. Metal oxide nano-sorbents have been widely used for the treatment of heavy metals such as cadmium and lead from wastewater. Metal oxide nanoparticles have a large surface area and are thus recognized as suitable adsorbents for water purification, especially heavy metal removal [19]. A number of metal oxides have been used for the removal of heavy metals, including ZnO [20], SnO_2 [21], Al-Ti_2O_6 [22], Fe_2O_3, Fe_3O_4 and Al_2O_3 [23-25], TiO_2 [26], MgO [27], ZrO_2 [28], CeO_2 [29], and so on.

The extract of grape products is obtained from chelating agents such as phenolic compounds and thus is a potent media for the preparation of nanoparticles. The literature review survey shows that the grape extract has been used for diverse nanostructures, including NiO nanoparticles [30], Ag nanoparticles [31-33], bimetallic Fe/Pd nanoparticles [34], gold nanoparticles [35], ZnO nanoparticles [36], graphene [37], and so on. In this study, we aim to use a green media prepared using grape extract for the preparation of SnO_2 nanoparticles. After synthesis, the as-prepared SnO_2 nanoparticles will be characterized based on their XRD, FE-SEM, TEM, BET, and DLS analyses. The final step of this study is the evaluation of the nanoparticles on the removal of Pb^{2+} and Cd^{2+} from wastewater.

2. Experimental

2.1. Materials and methods

All reagents, including bulk SnO_2, were purchased from Merck and Aldrich Companies and used without further purification. All yields refer to isolated products after purification. The powder X-ray diffraction patterns were measured with D8, Advance, Bruker, axs, and a diffractometer using Cu-$K\alpha$ irradiation. FE-SEM was taken using a Hitachi S-4160 photograph to examine the shape of the sample. The Dynamic light scattering (DLS) measurement was done using a Malvern Zetasizer Nano ZS (ZEN 3600) instrument. The grape extract was obtained from red grapes purchased from Isfahan province in Iran that were boiled in distilled water.

Nitrogen adsorption–desorption isotherms were collected at 77 K using Microtrac Belsorp (MINI II- Japan) equipment.

2.2. Preparation of SnO_2 nanoparticles in a grape extract media (Sample A)

First, 500 g of mashed grape sample was mixed with 250 ml of deionized water in a 500 ml beaker, boiled for 10 min, and filtered. Next, in a 250 ml beaker, $SnCl_2$ (20 mmol) was dissolved in 100 ml of ethanol containing 30 ml of grape extract (solution 1b). In a separate beaker, ammonia solution (30 ml) was diluted with water (50 ml) and 10 mlof grape extract (solution 2b). Solution 2b was slowly added dropwise to solution 1b under vigorous magnetic stirring. The mixture was continuously stirred for another 60 min. The resulting precipitate was filtered, washed with water several times, dried in an oven, and finally calcined at 500 °C for 3 h.

2.3. Preparation of SnO_2 nanoparticles (Sample B)

In a 250 ml beaker, $SnCl_2$ (20 mmol) was dissolved in 100 ml of ethanol (solution 1a). In a separate beaker, ammonia solution (30 ml) was diluted with water (50 ml) (solution 2a). Solution 2a was slowly added dropwise to solution 1a under vigorous magnetic stirring. The mixture was continuously stirred for another 60 min. The resulting precipitate was filtered, washed with water several times, dried in an oven, and finally calcined at 500 °C for 3h.

2.4. Adsorption experiment

$Pb(NO_3)_2$ and $CdSO_4.8H_2O$ were used as the source of lead and cadmium ions. Each of the solutions was prepared by dissolving the required amount of $Pb(NO_3)_2$/$CdSO_4.8H_2O$ in distilled water. An indirect batch equilibrium method was used for estimating the adsorption parameters at ambient conditions. Four different Cd^{2+} solutions with a concentration of 10, 20, 30, 40, 50, 60, 70, and 80 $mg.L^{-1}$ were prepared. The pH values of the solutions were adjusted from 3.5 to 7.5 using dilute HCl and NaOH. The samples were stirred in contact with SnO_2 under ambient conditions for 160 min. Each 20 min, the concentration of Cd^{2+} was determined using the atomic absorption technique (Varian Spectra A 250 Plus).

All the experiments for optimizing adsorbent dosage were done similarly to the above procedure. Different dosages of SnO_2, 0.01, 0.025, 0.05, 0.075, 0.1, and 0.2 g, while the Pb^{2+} and Cd^{2+} solutions were constant.

The removal percentage (R), adsorption capacities at time t (q_t), and adsorption capacities at equilibrium (q_e) were determined using Eqs. (1) to (3), respectively.

$$R = \frac{C_0 - C_t}{C_0} \times 100 \quad (1)$$

$$q_t = \frac{(C_0 - C_t) \times V}{m} \quad (2)$$

$$q_e = \frac{(C_0 - C_e) \times V}{m} \quad (3)$$

where C_0 ($mg.L^{-1}$) is the initial concentration of Cd^{2+}, C_t ($mg.L^{-1}$) is the concentration at time t (min), V (L) is the volume of solution, and m is the mass of adsorbent (g).

3. Results and discussion

3.1. SnO_2 Nanoparticles characterization

First, pure nanocrystals of SnO_2 nanoparticles were prepared from the precipitation reaction of Sn^{2+} solution in a green media of grape extract (Sample A) and without grape extract (Sample B). The XRD patterns of the calcined samples at 550 °C are shown in Fig. 1(a). The pattern of sample A consists of the tetragonal phase of SnO_2 (JCPDS Ref. Cod.: 01-077-0447, space group of P42/mnm) with characteristic peaks of 26.6, 33.9, 38.0, 51.8, 54.8, 61.9, 64.8, and 66.0 [2θ°]. Compared to A, sample B (without the extract) also shows tetragonal phase SnO_2 (JCPDS Ref. Cod.: 00-041-1445) with the characteristic peaks of 26.6, 33.9, 37.9, 51.8, 54.7, 61.9, 64.7, and 65.9 [2θ°].

The average crystallite size (D) was calculated from the XRD pattern using Scherrer's equation (Eq. (4)) as follows:

$$D = \frac{0.139}{\beta \mathrm{Cos}\theta} \quad (4)$$

where D is the crystal size (nm), θ is the Bragg angle, and β (in radian) is the entire width of the XRD peaks at half height.

The average crystallite size was estimated using Scherrer's equation [38] and found to be 41 and 49 nm, respectively, for Samples A and B.

The physical parameters of the two samples, including the specific surface area and pore diameter, were measured using BET and BJH methods, and the results are outlined in Fig. 1(c). The results indicate that the specific surface area and pore volume of SnO_2 decreased when the grape extract was missing.

The surface morphology of the SnO_2 nanoparticles prepared with and without the use of grape extract was investigated using FE-SEM (Fig. 1(b)) and TEM (Fig. 2) analyses. FE-SEM images reveal that both samples contain amorphous particles. However, the grape extract medium has a distinctive effect on homogeneity, as sample A shows more homogeneity and smaller particle size. TEM images confirmed the results

(a)

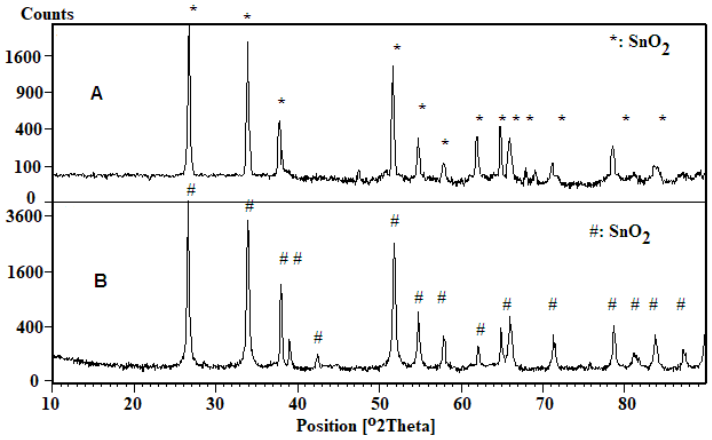

(b)

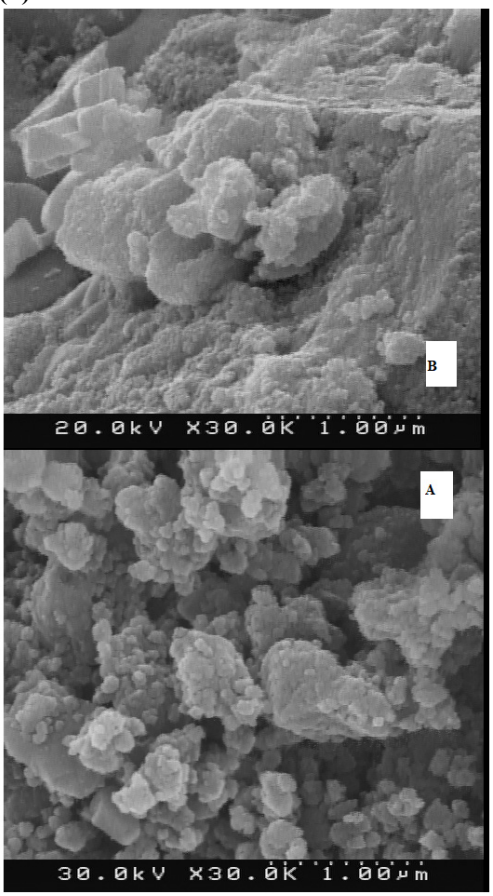

(c)

Sample	Specific surface area (m^2/g)		Pore diameter (nm)
	BET	BJH	BJH
A	47.08	46.25	6.49
B	39.54	39.25	4.89

Fig. 1. (a) XRD patterns, (b) FE-SEM images, and (c) the physical parameters of SnO_2 nanoparticles A (using grape extract) and B (without the use of grape extract).

of the FE-SEM analysis and indicated that the particles have diameters less than 100 nm. The particle size distribution curve of nanocomposites performed by the DLS technique is shown in Fig. 3. Before analysis, the sample was dispersed in ethanol (1 g in 25 ml) and sonicated for 30 min. The mean particle size of the nanoparticles determined by this method is approximately 45 nm (Sample A) and 78 nm (Sample B). The obtained results show that the particle size is more homogeneous when the grape extract is used to prepare the nanoparticles.

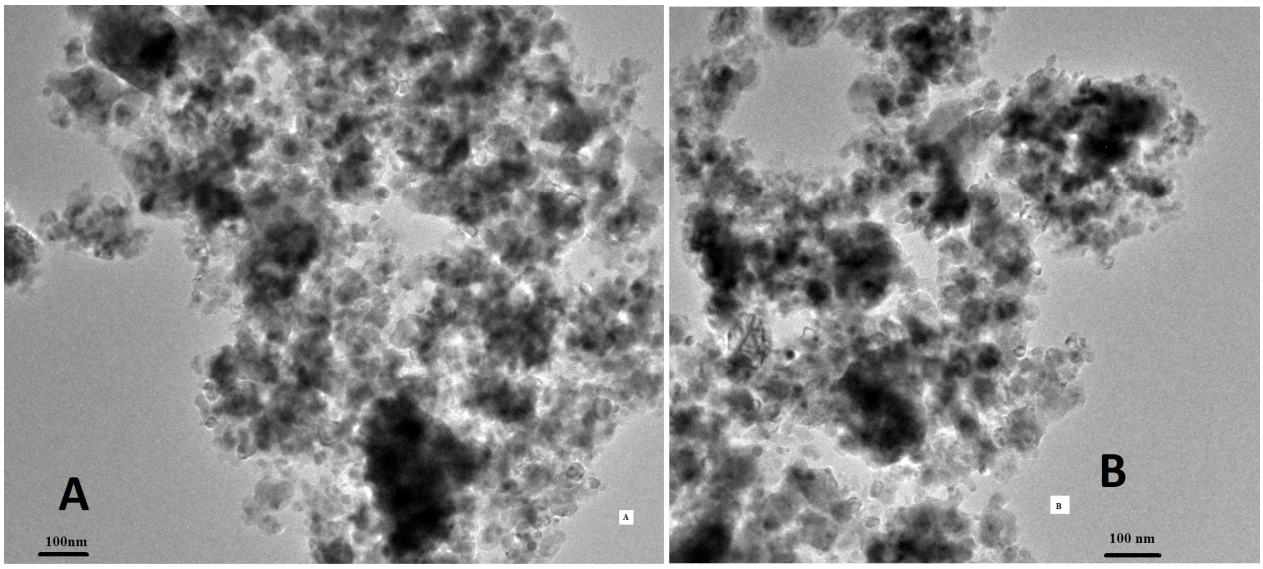

Fig. 2. HR-TEM images of SnO_2 nanoparticles A (using grape extract), and B (without grape extract).

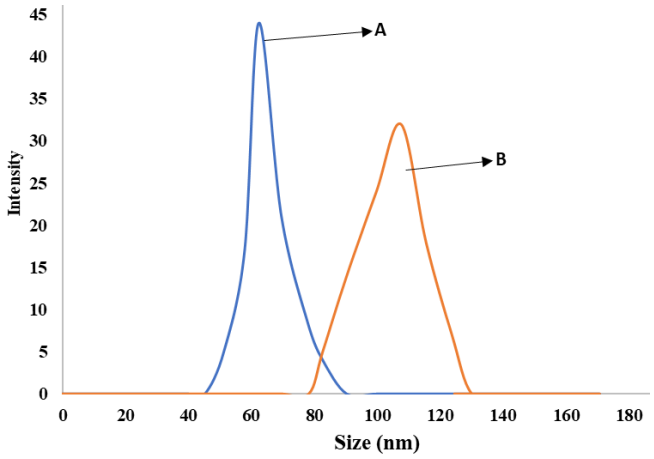

Fig. 3. DLS analysis of SnO_2 nanoparticles A (using grape extract), and B (without grape extract).

Grape extract is rich in cyanidin and delphinidin, two classes of phenolic compounds found in grape varieties. These compounds are able to form complex structures with tin ions. These complexes decompose in the calcination process and produce tin oxide at the nanoscale (Scheme 1) [39-41].

3.2. Removal of Pb^{2+} and Cd^{2+} ions

The effect of pH on Pb and Cd adsorption efficiency is shown in Fig. 4(A). As shown, the best adsorption efficiency occurs in a weak acidic media, pH = 6. As the pH changed from 3 to 7, the amount of Pb and Cd adsorption increased. Similar results have been reported by Ekubatsion *et al.* [42]. In general, in the adsorption process, the pH of an aqueous solution is a crucial control parameter because it determines the type of metal ion species and the charge level of the adsorbent. This will affect the reaction between adsorbent and adsorbate material. The effect of pH on the adsorption capacity is related to the chemical state of heavy metal in a solution at different amounts of pH, which can be a pure ionic

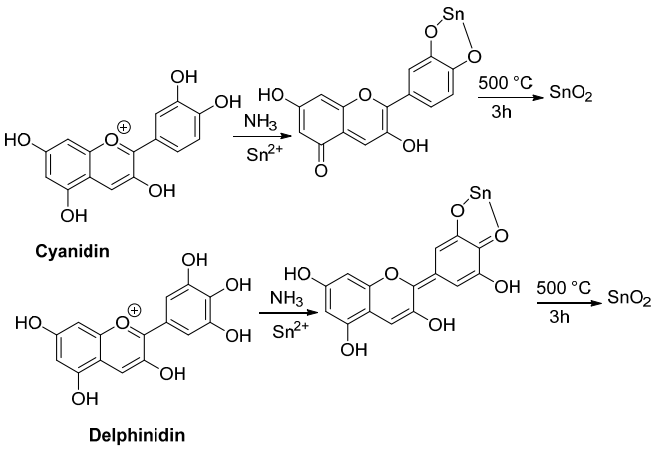

Scheme 1. Plausible interaction of cyanidin and delphinidin with Sn^{2+}: preparation of SnO_2 nanostructure.

form (Pb^{2+} and Cd^{2+}) in an acidic media or a hydroxyl-metal ($CdOH^{+}$) form in weak basic condition [42-44].

Next, the effect of contact time on the adsorption capacity was investigated. The results revealed that adsorption increased rapidly for the initial 90 min due to the high concentration of ions in the solution. After that, the filling of active nanoparticle sites and low Pb and Cd concentrations causes a slow adsorption process that follows a relatively linear trend (Fig. 4(B)).

Figs. 4(C) and 4(D) show the effect of SnO_2 dosages and the initial concentration of Pb and Cd on the adsorption values. It is known that at high Pb and Cd concentrations (higher than 30 ppm), the adsorption efficiency decreases because of the filling of active sites. On the other hand, the Pb and Cd removal increases up to 0.05 g of the SnO_2 dosage and consequently the adsorption efficiency decreases due to the agglomeration of SnO_2 species and reduction of active sites.

Temperature is another factor that affects heavy metal adsorption by adsorbents. Fig. 4(E) shows the effect of temperature on the adsorption of Pb and Cd ions. As can be seen, the adsorption efficiency decreases with increasing reaction temperature. The maximum adsorption was observed at 300 K at 93% for Cd and 97% for Pb. As revealed, the thermal energy of metal ions increased when temperature increased; thus, the contact probability of metal ions with vacant adsorbent sites increased. However, the mobility of ions and molecules increases at temperatures higher than 300 K, which breaks the adsorbent-metal ion interactions. This results in the metal ions being returned to the solution, reducing the adsorption efficiency [43]. The optimized conditions for adsorbing are a 30 ppm concentration of metal ions, ambient temperature, pH of 6, and 0.025 g of an adsorbent.

3.3. Kinetics investigation

The kinetic studies of Pb and Cd adsorption by SnO_2 as adsorbent were done using a linear distributions plot of pseudo-first-order ($\log(q_e\text{-}q_t)$ *vs.* t), pseudo-second-order (t/q_t *vs.* t), the Elovich model (q_t *vs.* $\ln t$), and Intra-particle diffusion (q_t *vs.* $t^{0.5}$) kinetic models at three different temperatures (283, 293, and 300 K) [45]. The equations and kinetic parameters of the models are summarized in Tables S1-S3 (Supplementary File). The correlation coefficient was used to match the experimental and predicted data of kinetic models. The corresponding parameters were calculated by drawing the linear diagrams of the equations. These charts are shown in Figs. S1-S4 (Supplementary File). A comparison of the correlation coefficients of different models shows that the Elovich model has the highest correlation coefficient, indicating that the adsorption mechanism is chemical

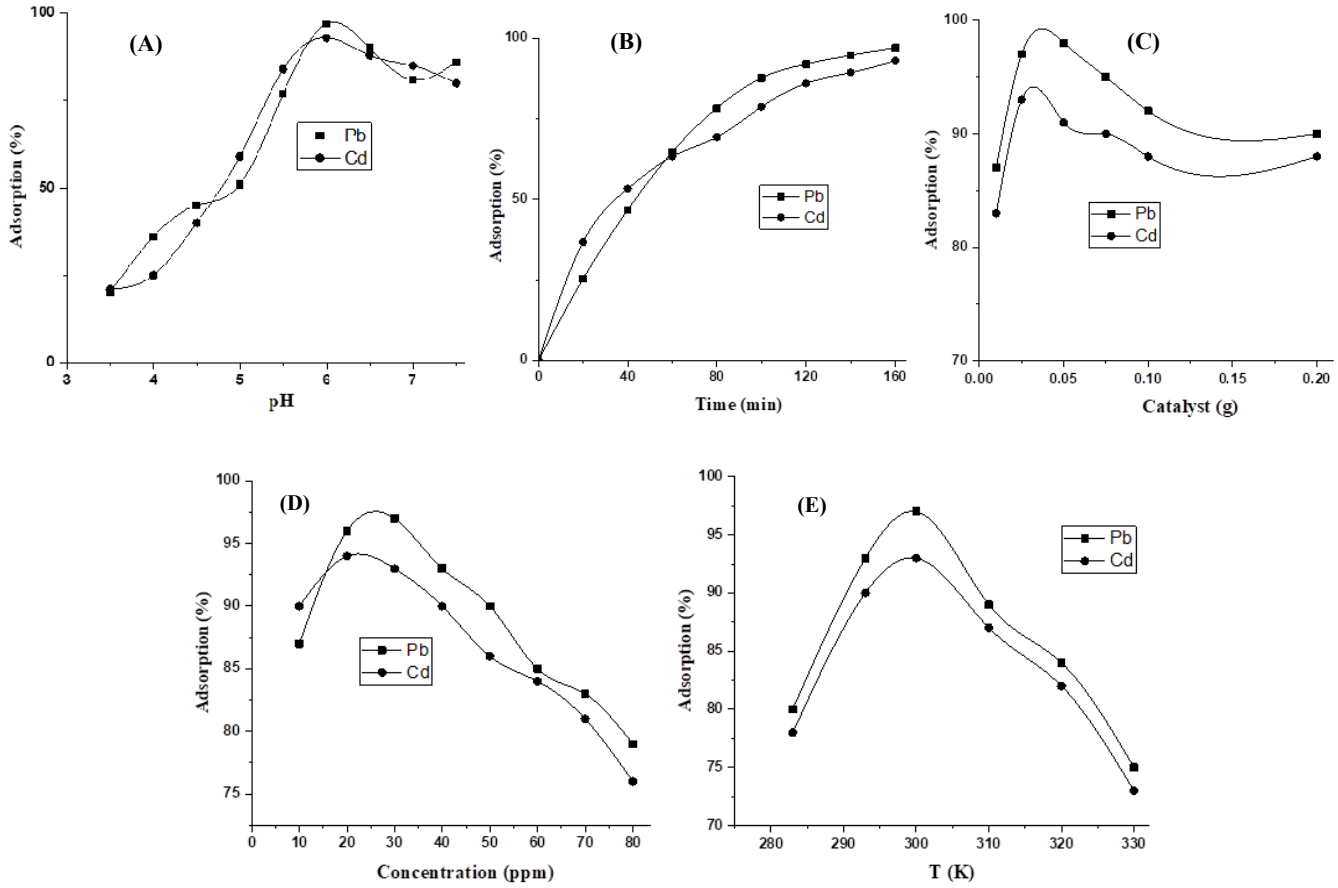

Fig. 4. Adsorption of Cd and Pb: effect of (A) pH (time: 160 min; SnO_2: 0.025 g; Cd: 40 ppm; r.t.); (B) contact time (pH: 6; time: 160 min; SnO_2: 0.025 g; Cd: 40 ppm; r.t.); (C) adsorbent dosage (pH: 6; time: 160 min; Cd: 40 ppm; r.t.); (D) initial concentration (pH: 6; time: 160 min; SnO_2: 0.025 g; r.t.); and (E) temperature (pH: 6; time: 160 min; SnO_2: 0.025 g; Cd: 40 ppm).

adsorption. Studies also show that the calculated q_e differs from first-order quadratic and pseudo-second kinetic models.

3.4. Thermodynamic investigations

Data obtained from the thermodynamic study were used to determine the Gibbs free energy, enthalpy, and entropy of the system. The change in the Gibbs free energy for lead and cadmium ions at four different temperatures (300-330 K) was obtained through the relationships between ΔG, ΔH, ΔS, and $\mathrm{Ln}K_c$ in Eqs. (5) and (6), shown in Table 1. ΔH and ΔS are obtained by drawing the $\mathrm{Ln}K_c$ diagram against $1/T$ (Fig. 5).

$$\Delta G^0 = -8.314T\ln K_c \qquad K_c = \frac{q_e}{C_e} \tag{5}$$

$$\ln K_c = \frac{\Delta S^0}{RT} - \frac{\Delta H^0}{RT} \tag{6}$$

where K_c (L.mg^{-1}) is the equilibrium constant, and T is the absolute temperature (K).

The thermodynamic parameters ΔG^0, ΔH^0, and ΔS^0 are shown in Table 1. The negative values of ΔG^0 represent the spontaneous of the adsorption processes. Additionally, the values of ΔG in the present study were relatively close to zero, which indicates that the trend is close to the equilibrium. The results of this study indicate that the reaction occurs with the bonding of metal ions to the surface of nanomaterials. The values of ΔH and ΔS are shown in Table 1. Negative values of ΔH and ΔS reveal that the adsorption reaction is exothermic [45].

Table 1. Thermodynamic parameters for the adsorptive removal of Pb and Cd ions using SnO_2 nanoparticles.

ΔS^0 (J.mol^{-1})		ΔH^0 (kJ.mol^{-1})	
Pb	**Cd**	**Pb**	**Cd**
-188.8	-128.4	-63.0	42.95
T (K)		ΔG^0 (kJ.mol^{-1})	
		Pb	**Cd**
300		-6.38	-4.16
310		-3.04	-2.54
320		-1.97	-1.59
330		-0.493	-0.211

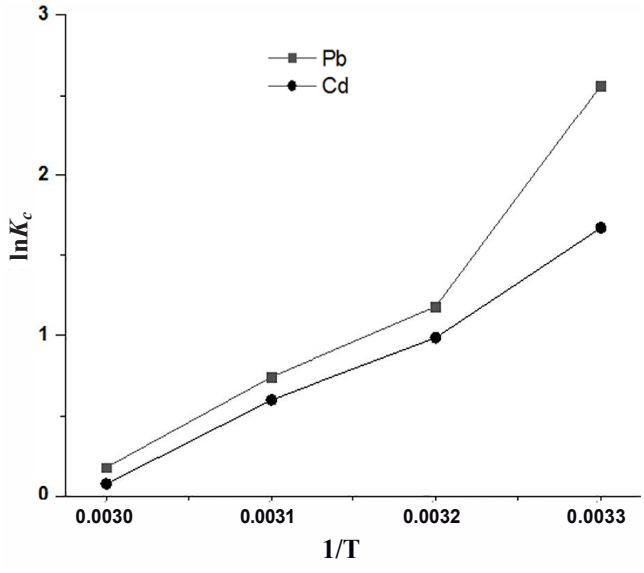

Fig. 5. Plots of lnK_c *vs.* 1/*T*.

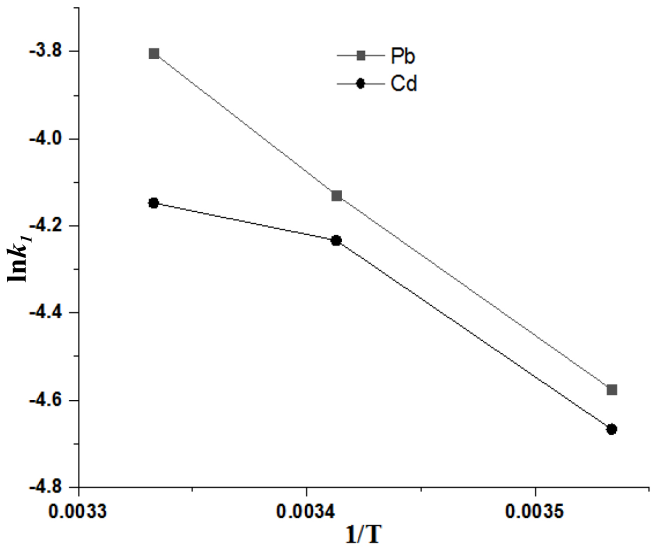

Fig. 6. Plots of lnk_1 *vs.* 1/*T*.

3.5. Activation energy investigations

The results of kinetic studies showed that the adsorption of lead and cadmium ions depends on the time and temperature. Generally, the adsorption increases with time and decreases with temperature increase. Data from kinetic studies at different temperatures are used to determine the activation energy of the adsorption using the Arrhenius equation ($k = A\ e^{-E_a/RT}$). In this equation, k is the rate constant, A is the Arrhenius constant, E_a is the activation energy, R is the gas constant (8.314 J.mol^{-1}), and T is the reaction temperature in Kelvin. The values for k are calculated by plotting zero as well as first and second-order kinetics (Figs. S5, S6, and S7 in the Supplementary File). The calculated values of rate constants, correlation coefficient of zero, and first and second-order kinetics are summarized in Table S4 (Supplementary File). According to the higher correlation coefficient results of the first order, this model was chosen as the rate equation of the adsorption reaction. Thus, the parameters of the Arrhenius equation were determined from the values of first-order kinetics (Fig. 6, Table 2). From the drawing of the ln$k$ *vs.* 1/*T*, we can calculate the parameters of the Arrhenius equation (Fig. 6). In this case, the slope of the line is equal to $-E_a/R$ [46]. The results are summarized in Table 2.

Table 2. Parameters of the Arrhenius equation (lnk_1 *vs.* 1/*T*).

E_a (kJ.mol^{-1})		*A*		R^2	
Pb	**Cd**	**Pb**	**Cd**	**Pb**	**Cd**
32.02	22.25	8208.09	123.08	0.9994	0.937

Studies have shown that the activation energy required to adsorb Pb ions is higher than those required for Cd adsorption. The values of activation energy reflect the fact that the adsorption of these elements is accomplished by chemical adsorption

3.6. Reusability investigations

For the reusability of SnO_2 nanoparticles, the solution was centrifuged and decanted to remove the adsorbent. Subsequently, a solution of 1 M acetic acid was added, and the suspension was stirred for 1 h to release the Cd and Pb ions from the adsorbent surface. The results of four repetitions of the recovery experiment are shown in Fig. 7. The result showed that the adsorbent retained about 90% of its initial efficiency even after four cycles.

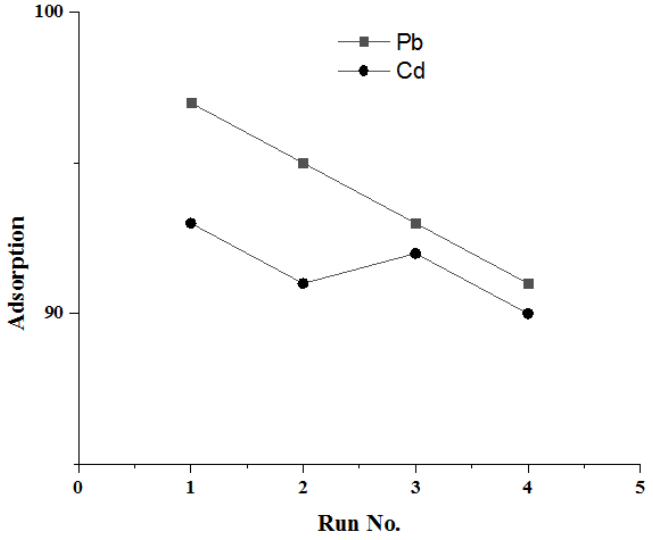

Fig. 7. Reusability of SnO_2 nanoparticles.

3.7. Comparison results

Comparatively, nanoparticles prepared without the use of grape extract show lower adsorption capacity than those prepared in a grape extract media. In addition, SnO_2 nanoparticles have a higher adsorption capacity than SnO_2 bulk materials. The grape extract performs a non-toxic and environmentally friendly green preparation procedure for the SnO_2 nanoparticle. Accordingly, this work is beneficial to methods that use toxic solvents and reagents to prepare nanoparticles. In addition, SnO_2 nanoparticles prepared using grape extract have higher adsorption capacity, which adsorbed heavy metals more effectively. Moreover, the results we obtained agree well with those reported in the literature and, in some cases, are much higher than other adsorbents (Table 3).

4. Conclusion

The SnO_2 nanoparticles were synthesized using a simple and inexpensive method and were analyzed by XRD, FESEM, TEM, BET, and DLS analyses. The capability of SnO_2 nanoparticles was evaluated in the adsorption of Pb^{2+} and Cd^{2+} ions. The effect of different factors on adsorption, such as pH, adsorbent amount, adsorbate concentration, and temperature, was investigated. The best conditions for adsorbing were found to be a 30 ppm concentration of metal ions, ambient temperature, pH of 6, and 0.025 g of an adsorbent. Kinetic studies were carried out to determine the adsorption mechanism. A comparison of the correlation coefficients of different models shows that the Elovich model has the highest correlation coefficient, indicating that the adsorption mechanism is chemical adsorption. The thermodynamic parameters ΔG, ΔH, and ΔS, as well as the activation energy of the adsorption process, were calculated. The negative values of ΔG represent the spontaneousness of the adsorption process. The negative values of the parameters ΔH and ΔS represent the exothermic nature of the adsorption. The values associated with activation energy reflect the fact that the adsorption of these elements is accomplished through chemical adsorption. This method could be applied for the preparation of different metal oxides in the nanoscale because it has several advantages, such as using environmentally friendly media and removing hazardous and toxic chemicals

Table 3. Comparison results with the literature.

Adsorbent	Heavy metals removal (%)	Ref.
Bulk SnO_2	Cd (81%), Pb (84%)	This work
SnO_2 nanoparticles (NPs) (prepared without the use of grape extract)	Cd (85%), Pb (89%)	This work
SnO_2 NPs (prepared using grape extract)	Cd (93%), Pb (97%)	This work
SnO_2 NPs Synthesized using Vitex agnus-castus fruit extract	Co (94%)	[47]
SnO_2 NPs	Zn (83%)	[48]
AgNPs-Doped SnO_2	Cd and Pb (over 96.9%)	[49]
SnO_2 NPs	Cd and Pb (below 70%)	[50]
SnO_2 Crosslinked-chitosan	Cd (95.6%), Hg (94.2%)	[51]
PMMA/SnO_2 Nanocomposites	Cr (Over 90%)	[52]

Acknowledgment

We thank the Najafabad Branch, Islamic Azad University Research Council, for partially supporting this research.

Disclosure statement

No potential conflict of interest was reported by the authors.

References

[1] Karmaoui, M., Jorge, A. B., McMillan, P. F., Aliev, A. E., Pullar, R. C., Labrincha, J. A., & Tobaldi, D. M. (2018). One-Step Synthesis, Structure, and Band Gap Properties of SnO_2 Nanoparticles Made by a Low Temperature Nonaqueous Sol-Gel Technique. *ACS Omega 3*(10), 13227-13238. https://doi.org/10.1021/acsomega.8b02122

[2] Naz, S., Javid, I., Konwar, S., Surana, K., Singh, P. K., Sahni, M., & Bhattacharya, B. (2020). A Simple Low Cost Method for Synthesis of SnO_2 Nanoparticles and Its Characterization. *SN Applied Sciences, 2*, 975. https://doi.org/10.1007/s42452-020-2812-2

[3] Dehbashi, M., Aliahmad, M., Shafiee, M. R. M., & Ghashang, M. (2013). SnO_2 Nanoparticles: Preparation and Evaluation of Their Catalytic Activity in the Oxidation of Aldehyde Derivatives to Their Carboxylic Acid and Sulfides to Sulfoxide Analogs. *Phosphorus, Sulfur, and Silicon and the Related Elements, 188*(7), 864-872. https://doi.org/10.1080/10426507.2012.717139

[4] Dehbashi, M., Aliahmad, M., Shafiee, M. R. M., & Ghashang, M. (2013). Nickel-Doped SnO_2 Nanoparticles: Preparation and Evaluation of Their Catalytic Activity in the Synthesis of 1-Amidoalkyl-2-Naphtholes. Synthesis and Reactivity in Inorganic, Metal-Organic, and Nano-Metal Chemistry, 43(9), 1301-1306. https://doi.org/10.1080/15533174.2012.757753

[5] Sathishkumar, M., & Geethalakshmi, S. (2020). Enhanced Photocatalytic and Antibacterial Activity of Cu: SnO_2 Nanoparticles Synthesized by Microwave Assisted Method. *Materials Today: Proceedings 20*(Part 1), 54-63. https://doi.org/10.1016/j.matpr.2019.08.246

[6] Xuemei, P., Dan, Z., & Haitao, C., Preparation Method of Efficient Single-Phase SnO_2 Photocatalyst, CN105749902A (issued July 13, 2016).

[7] Suriya, P., Prabhu, M., Satheesh Kumar, E., & Jagannathan, K. (2022). Effect of Ag Doping on Structural, Optical, Complex Impedance and Photovoltaic Properties of SnO_2 Nanoparticles Prepared by Co-Precipitation Method for Dye Sensitized Solar Cell Application. *Optik ,260*, 168971. https://doi.org/10.1016/j.ijleo.2022.168971

[8] Godlaveeti, S. K., Somala, A. R., Sana, S. S., Ouladsmane, M., Ghfar, A. A., & Nagireddy, R. R. (2022). Evaluation of pH Effect of Tin Oxide (SnO_2) Nanoparticles on Photocatalytic Degradation, Dielectric and Supercapacitor Applications. *Journal of Cluster Science, 33*, 1635-1644. https://doi.org/10.1007/s10876-021-02092-7

[9] Patel, G. H., Chaki, S. H., Kannaujiya, R. M., Parekh, Z. R., Hirpara, A. B., Khiman, A. J., & Deshpande, M. P. (2021). Sol-Gel Synthesis and Thermal Characterization of SnO_2 Nanoparticles. *Physica B: Condensed Matter, 613*, 412987. https://doi.org/10.1016/j.physb.2021.412987

[10] Ghashang, M., Mansoor, S. S., Mohammad Shafiee, M. R., Kargar, M., Najafi Biregan, M., Azimi, F., & Taghrir, H. (2016). Green Chemistry Preparation of MgO Nanopowders: Efficient Catalyst for the Synthesis of Thiochromeno[4,3-b]pyran and Thiopyrano[4,3-b]pyran Derivatives. *Journal of Sulfur Chemistry, 37*(4), 377-390. https://doi.org/10.1080/17415993.2016.1149856

[11] Ghashang, M., Mansoor, S. S., Shams Solaree, L., & Sharifian-Esfahani, A. (2016). Multi-Component, One-Pot, Aqueous Media Preparation of Dihydropyrano[3,2-c] chromene Derivatives Over MgO Nanoplates as An Efficient Catalyst. *Iranian Journal of Catalysis, 6*(3), 237-243. https://journals.iau.ir/article_560293.html

[12] Ghashang, M., Kargar, M., Shafiee, M. R. M., Mansoor, S. S., Fazlinia, A., & Esfandiari, H. (2015). CuO Nano-Structures Prepared in Rosmarinus Officinalis Leaves Extract Medium: Efficient Catalysts for the Aqueous Media Preparation of Dihydropyrano[3,2-c]chromene Derivatives. *Recent Patents on Nanotechnology, 9*(3), 204-211. https://doi.org/10.2174/1872210510999151126110657

[13] Shafiee, M. R. M., Kargar, M., Hashemi, M. S., & Ghashang, M. (2016). Green Synthesis of $NiFe_2O_4$/Fe_2O_3/CeO_2 Nanocomposite in a Walnut Green Hulls Extract Medium: Magnetic Properties and Characterization. *Current Nanoscience, 12*(5), 645-649. https://doi.org/10.2174/1573413712666160513124809

[14] Shafiee, M. R. M., Kargar, M., & Ghashang, M. (2018). Characterization and Low-Cost, Green Synthesis of Zn^{2+} Doped MgO Nanoparticles. *Green Processing and Synthesis, 7*(3), 248-254. https://doi.org/10.1515/gps-2016-0219

[15] Mobinikhaledi, A., Yazdanipour, A., & Ghashang, M. (2016). Green Chemistry Preparation of MgO Grit Like Nanostructures: Efficient Catalyst for the Synthesis of 4*H*-Pyrans and α,α′-Bis(substituted-benzylidene) cycloalkanone Derivatives. *Green Processing and Synthesis, 5*(3), 289-295. https://doi.org/10.1515/gps-2015-0136

[16] Burakov, A. E., Galunin, E. V., Burakova, I. V., Kucherova, A. E., Agarwal, S., Tkachev, A. G., & Gupta, V. K. (2018). Adsorption of Heavy Metals on Conventional and Nanostructured Materials for Wastewater Treatment Purposes: A Review. *Ecotoxicology and Environmental Safety, 148*, 702-712. https://doi.org/10.1016/j.ecoenv.2017.11.034

[17] Afroze, S., & Sen, T. K. (2018). A Review on Heavy Metal Ions and Dye Adsorption from Water by Agricultural Solid Waste Adsorbents. *Water, Air, & Soil Pollution, 229*, 225. https://doi.org/10.1007/s11270-018-3869-z

[18] Fu, F., & Wang, Q. (2011). Removal of Heavy Metal Ions from Wastewaters: A Review. *Journal of Environmental Management, 92*(3), 407-418. https://doi.org/10.1016/j.jenvman.2010.11.011

[19] Hua, M., Zhang, S., Pan, B., Zhang, W., Lv, L., & Zhang, Q. (2012). Heavy Metal Removal from Water/Wastewater by Nanosized Metal Oxides: A Review. *Journal of Hazardous Materials, 211-212*, 317-331. https://doi.org/10.1016/j.jhazmat.2011.10.016

[20] Le, A. T., Pung, S.-Y., Sreekantan, S., Matsuda, A., & Huynh, D. P. (2019). Mechanisms of Removal of Heavy Metal Ions by ZnO Particles. *Heliyon 5*(4), e01440. https://doi.org/10.1016/j.heliyon.2019.e01440

[21] Kumar, K. Y., Muralidhara, H. B., Nayaka, Y. A., Balasubramanyam, J., & Hanumanthappa, H. (2013). Low-Cost Synthesis of Metal Oxide Nanoparticles and Their Application in Adsorption of Commercial Dye and Heavy Metal Ion in Aqueous Solution. *Powder Technology, 246*, 125-136. https://doi.org/10.1016/j.powtec.2013.05.017

[22] Sunil, K., Karunakaran, G., Yadav, S., Padaki, M., Zadorozhnyy, V., & Pai, R. K. (2018). Al-Ti_2O_6 A Mixed Metal Oxide Based Composite Membrane: A Unique Membrane for Removal of Heavy Metals. *Chemical Engineering Journal, 348*, 678-684. https://doi.org/10.1016/j.cej.2018.05.017

[23] Chang, Y.-Y., Lee, S.-M., & Yang, J.-K. (2009). Removal of As(III) and As(V) by Natural and Synthetic Metal Oxides. *Colloids and Surfaces A: Physicochemical*

and Engineering Aspects, 346(1-3), 202-207. https://doi.org/10.1016/j.colsurfa.2009.06.017

[24] Chen, Y. H., & Li, F. A. (2010). Kinetic Study on Removal of Copper (II) Using Goethite and Hematite Nano-Photocatalysts. *Journal of Colloid and Interface Science, 347*(2), 277-281. https://doi.org/10.1016/j.jcis.2010.03.050

[25] Hu, J., Chen, G. H., & Lo, I. M. C. (2005). Removal and Recovery of Cr(VI) rom Wastewater by Maghemite Nanoparticles. *Water Research, 39*(18), 4528-4236. https://doi.org/10.1016/j.watres.2005.05.051.

[26] Giammar, D. E., Maus, C. J., & Xie, L. Y. (2007). Effects of Particle Size and Crystalline Phase on Lead Adsorption to Titanium Dioxide Nanoparticles. *Environmental Engineering Science, 24*(1), 85-95. https://doi.org/10.1089/ees.2007.24.85

[27] Madzokere, T. C., & Karthigeyan, A. (2017). Heavy Metal Ion Effluent Discharge Containment Using Magnesium Oxide (MgO) Nanoparticles. *Materials Today: Proceedings, 4*(1), 9-18. https://doi.org/10.1016/j.matpr.2017.01.187

[28] Hristovski, K. D., Westerhoff, P. K., Crittenden, J. C., & Olson, L. W. (2008). Arsenate Removal by Nanostructured ZrO_2 Spheres. *Environmental Science & Technology, 42*(1), 3786-3790. https://doi.org/10.1021/es702952p

[29] Colón, J., Casals, E., González, E., Puntes, V., Sánchez, A., & Font, X. (2010). Chromium VI Adsorption on Cerium Oxide Nanoparticles and Morphology Changes During the Process. *Journal of Hazardous Materials, 184*(1-3), 425-431. https://doi.org/10.1016/j.jhazmat.2010.08.052

[30] Hussein, B. Y., & Mohammed, A. M. (2021). Biosynthesis And Characterization of Nickel Oxide Nanoparticles by Using Aqueous Grape Extract and Evaluation of Their Biological Applications. *Results in Chemistry, 3*, 100142. https://doi.org/10.1016/j.rechem.2021.100142

[31] Bastos-Arrieta, J., Florido, A., Pérez-Ràfols, C., Serrano, N., Fiol, N., Poch, J., & Villaescusa, I. (2018). Green Synthesis of Ag Nanoparticles Using Grape Stalk Waste Extract for the Modification of Screen-Printed Electrodes. *Nanomaterials 8*(11), 946. https://doi.org/10.3390/nano8110946

[32] Dziwoń, K., Pulit-Prociak, J., & Banach, M. (2015). Green Technologies in Obtaining Nanomaterials - Using White Grapes (*Vitis vinifera*) in the Processes for the Preparation of Silver Nanoparticles. *Chemik ,69*(1), 33-38.

[33] Said, M. I., & Othman, A. A. (2019). Fast Green Synthesis of Silver Nanoparticles Using Grape Leaves Extract. *Materials Research Express, 6*(5), 055029. https://doi.org/10.1088/2053-1591/ab0481

[34] Luo, F., Yang, D., Chen, Z., Megharaj, M., & Naidu, R. (2016). Characterization of Bimetallic Fe/Pd Nanoparticles by Grape Leaf Aqueous Extract andIdentification of Active Biomolecules Involved in the Synthesis. *Science of The Total Environment, 562*, 526-532. https://doi.org/10.1016/j.scitotenv.2016.04.060

[35] Krishnaswamy, K., Vali, H., 7 Orsat, V. (2014). Value-Adding to Grape Waste: Green Synthesis of Gold Nanoparticles. *Journal of Food Engineering, 142*, 210-220. https://doi.org/10.1016/j.jfoodeng.2014.06.014

[36] Hussein, B. Y., & Mohammed, A. M. (2021). Green Synthesis of ZnO Nanoparticles in Grape Extract: Their Application as Anti-cancer and Anti-bacterial. *Materials Today: Proceedings, 42*(Part 3), A18-A26. https://doi.org/10.1016/j.matpr.2021.03.729

[37] Yaragalla, S., Rajendran, R., Jose, J., AlMaadeed, M. A., Kalarikkal, N., & Thomas, S. (2016). Preparation and Characterization of Green Graphene Using Grape Seed Extract for Bioapplications. *Materials Science and Engineering: C, 65*, 345-353. https://doi.org/10.1016/j.msec.2016.04.050

[38] Khosravian, P., Ghashang, M., & Ghayoor, H. (2017). Effective Removal of Penicillin from Aqueous Solution Using Zinc Oxide/Natural-Zeolite Composite Nano-Powders Prepared Via Ball Milling Technique. Recent Patents on Nanotechnology, 11(2), 154-164. https://doi.org/10.2174/1872210511666170105141550

[39] Ekubatsion, L. H., Thriveni, T., & Ahn, J. W. (2021). Removal of Cd^{2+} and Pb^{2+} from Wastewater through Sequent Addition of KR-Slag, $Ca(OH)_2$ Derived from Eggshells and CO_2 Gas. *ACS Omega 6*(42), 27600-27609. https://doi.org/10.1021/acsomega.1c00946

[40] Al-Mur, B. A. (2023). Green Zinc Oxide (ZnO) Nanoparticle Synthesis Using Mangrove Leaf Extract from Avicenna marina: Properties and Application for the Removal of Toxic Metal Ions (Cd^{2+} and Pb^{2+}). *Water, 15*(3), 455. https://doi.org/10.3390/w15030455

[41] Khorram Abadi, V., Habibi, D., Heydarib, S., & Ariannezhad, M. (2023). The Effective Removal of Ni^{2+}, Cd^{2+}, and Pb^{2+} from Aqueous Solution by Adenine-based Nanoadsorbent. *RSC Advances, 13*, 5970-5982. https://doi.org/10.1039/D2RA07230K

[42] Gharib, A., Faezizadeh, Z., & Godarzee, M. (2013). Treatment of Diabetes in the Mouse Model by Delphinidin and Cyanidin Hydrochloride in Free and Liposomal Forms. *Planta Medica, 79*(17), 1599-1604. https://doi.org/10.1055/s-0033-1350908

[43] Sabra, A., Netticadan, T., & Wijekoon, C. (2021). Grape Bioactive Molecules, and the Potential Health Benefits in Reducing the Risk of Heart Diseases. *Food Chemistry: X, 12*, 100149. https://doi.org/10.1016/j.fochx.2021.100149

[44] Šikuten, I., Štambuk, P., Andabaka, Ž., Tomaz, I., Marković, Z., Stupić, D., Maletić, E., Kontić, J. K.,

& Preiner, D. (2020). Grapevine as a Rich Source of Polyphenolic Compounds. *Molecules 25*(23), 5604. https://doi.org/10.3390/molecules25235604

[45] Manzoor, K., Ahmad, M., Ahmad, S., & Ikram, S. (2019). Removal of Pb(II) and Cd(II) from Wastewater Using Arginine Crosslinked Chitosan-Carboxymethyl Cellulose Beads as Green Adsorbent. *RSC Advances, 9*(14),7890-7892. https://doi.org/10.1039/C9RA00356H

[46] Iftikhar, A. R., Bhatti, H. N., Hanif, M. A., & Nadeem, R. (2009). Kinetic and Thermodynamic Aspects of Cu(II) and Cr(III) Removal from Aqueous Solutions Using Rose Waste Biomass. *Journal of Hazardous Materials, 161*(2-3), 941-947. https://doi.org/10.1016/j.jhazmat.2008.04.040

[47] Ebrahimian, J., Mohsennia, M., & Khayatkashani, M. (2020). Photocatalytic-Degradation of Organic Dye and Removal of Heavy Metal Ions Using Synthesized SnO_2 Nanoparticles by *Vitex Agnus-Castus* Fruit Via a Green Route. Materials Letters, 263, 127255. https://doi.org/10.1016/j.matlet.2019.127255

[48] Ahmed, M., Elektorowicz, M., & Hasan, S. W. (2019). GO, SiO_2, and SnO_2 Nanomaterials as Highly Efficient Adsorbents for Zn^{2+} from Industrial Wastewater - A Second Stage Treatment to Electrically Enhanced Membrane Bioreactor. *Journal of Water Process Engineering, 31*, 100815. https://doi.org/10.1016/j.jwpe.2019.100815

[49] Feng, L., He, R., Li, H., Wang, J., Chen, S., Liu, N., Liu, G., Wang, X., & Zhao, G. (2023). An Efficient Pretreatment Method Based on Agnps-Doped SnO_2 Photocatalyst for the Accurate Detection of Heavy Metals in Organic-Rich Water Samples. *Chemosphere, 344*, 140270. https://doi.org/10.1016/j.chemosphere.2023.140270

[50] Kumar, K. Y., Vinuth Raj, T. N., Archana, S., Benaka Prasad, S. B., Olivera, S., & Muralidhara, H. B. (2016). SnO_2 Nanoparticles as Effective Adsorbents for the Removal of Cadmium and Lead from Aqueous Solution: Adsorption Mechanism and Kinetic Studies. *Journal of Water Process Engineering, 13*, 44-52. https://doi.org/10.1016/j.jwpe.2016.07.007

[51] Mahmoud, M. E., Abdelwahab, M. S., & Ibrahim, G. A. A. (2022). The Design of SnO_2-Crosslinked-Chitosan Nanocomposite for Microwave-Assisted Adsorption of Aqueous Cadmium and Mercury Ions. *Sustainable Chemistry and Pharmacy, 28*, 100731. https://doi.org/10.1016/j.scp.2022.100731

[52] Alkayal, N. S. (2022). Fabrication of Cross-linked PMMA/SnO_2 Nanocomposites for Highly Efficient Removal of Chromium (III) from Wastewater. Polymers 14(10), 2101. https://doi.org/10.3390/polym14102101

Additional information

Correspondence and requests for materials should be addressed to S. Jabbarzare.

HOW TO CITE THIS ARTICLE

Jabbarzare, S. (2023). Heavy Metal Removal Using SnO_2 Nanoparticles Prepared in a Grape Extract Media. *J. Part. Sci. Technol. 9(2) 51-61.*

DOI: 10.22104/JPST.2023.6385.1236
URL: https://jpst.irost.ir/article_1336.html